Synthesis and characterization of SiO₂–La₂O₃ gels obtained in a water-free environment

Waldemar Nowicki · Ganna Rypka ·
Adriana Kawałko · Agnieszka Tolińska ·
Piotr Kirszensztejn

Abstract SiO₂–La₂O₃ binary oxide system was prepared by the sol–gel method without addition of strong polar solvents (e.g. water, alcohol) to the initial system. Changes in the surface and gel network structure were described as a function of the type and concentration of the second component that is lanthanum oxide. A series of samples with Si to La molar ratios of 1:0.1, 1:0.25, 1:0.5, and 1:1 were characterised by XRD, TG–TA, FTIR, and low-temperature nitrogen adsorption measurements. Results of the investigation showed that higher amounts of the lanthanum component in the binary oxide gel system led to a completely changed morphology of the porous structure of the surface gels obtained in a non-aqueous medium.

Introduction

Rare earth elements are attractive materials for industry and play an important role in a number of current technologies as active components. A number of applications of rare earth-activated materials have been developed, for instance in optical technologies, that have led expected to construction of photonic devices [1], catalytic [2–6] and photoluminescence [7] systems. In this connection, the low-temperature sol–gel synthesis has been recently of considerable scientific and technological interest [8].

W. Nowicki (✉) · A. Kawałko · A. Tolińska · P. Kirszensztejn
Faculty of Chemistry, Adam Mickiewicz University,
Grunwaldzka 6, 60-780 Poznań, Poland
e-mail: waldek@amu.edu.pl

G. Rypka
Department of Organics Products, Institute of Chemistry and
Chemical Technology, Lviv Polytechnic, Bandera 12,
79013 Lviv, Ukraine

Indeed, starting from liquid molecular precursor it is possible to produce via hydrolysis–condensation reactions, a great variety of unusual gel oxide materials whose chemical composition and structure can be tailored by the chemical design of molecular precursors and synthesis parameters. Furthermore, low temperature synthesis not only reduces the cost of processing but also helps solving problems related to volatilization [9] and permits production of materials with high surface area and high purity. The standard sol–gel technique for obtaining inorganic materials, involves hydrolysis of mixed-metal alkoxides and polycondensation of the forming compounds, which requires that polar solvents, strong inorganic acids and water should be used as necessary components of a sol–gel system [10]. The major problem is to control the reaction rates in sol–gel methods based on the hydrolysis–condensation reaction. The rates of these reactions are generally too fast, which leads to a reduction of microstructural control of the final product. An attractive solution is provided by nonhydrolitic sol–gel conditions [11–13]. An alternative approach that opens up new possibilities in sol–gel chemistry is to perform the sol–gel process without adding water to the initial system. It is particularly important for multicomponent systems in which the precursors applied differ much in the rate of hydrolysis. Recently, we have proposed a new procedure for the synthesis of binary oxide gel systems of well-developed surface area, containing both silica and tin components, in water free conditions [14]. By controlling the hydrolysis through a slow release of esterification water, we avoided precipitation of large agglomerates of the component but a higher rate of hydrolysis could be maintained. As a result, we could expect that the second component should be uniformly dispersed in a binary gel

and correlate with the surface acidity/basicity of a catalyst (article in preparation). This method permits production of organic–inorganic hybrid materials from water-insoluble components. The use of improved materials makes it possible to design new products and improved processes. The aim of the present study is to propose a method for the synthesis of SiO_2–La_2O_3 gels with the use of three compounds (tetraethylorthosilicate, lanthanum acetate, AcOH) in water-free environment and to establish if the parameters such as surface area, pore volume, and the amorphous structure can be to some extent independently controlled. The main reason for taking up the studies was the literature information that lanthanide oxides can act as promoters of texture, in particular by reducing the thermal sintering of the system to which they are added [15, 16]. On the other hand, lanthanum oxide itself has been shown to be a catalyst for many chemical reactions [17–19]. The above information and the fact that we have much experience in the synthesis of oxide systems through sol–gel processes in an anhydrous conditions has stimulated us to take up this issue. The choice of SiO_2 was dictated by its wide applications as a carrier material, which is related to its inert nature and large surface area [20, 21].

Experimental

Synthesis of binary oxide gel system

A series of SiO_2–La_2O_3 samples with the La/Si molar ratios of 0.1, 0.25, 0.5 and 1.0 were synthesised by the sol–gel technique with the use of tetraethylorthosilicate (TEOS) obtained from ABCR GmbH & Co. KG and $La(CH_3COO)_3$ synthesised in our laboratory. The samples were marked according to the increasing content of lanthanum as SiLa 0.1, SiLa 0.25, SiLa 0.5 and SiLa 1.0, respectively. The SiO_2 gel was synthesised by adding 100 cm^3 of TEOS (0.44 mol) into 300 cm^3 of anhydrous acetic acid (5.25 mol) to an Erlenmeyer flask under stirring. The obtained homogeneous solution was closed in a glass vessel and heated under autogenic pressure at 353 K for at least 48 h. The binary oxide gel system was obtained by mixing the appropriate amounts of precursors that were TEOS and $La(CH_3COO)_3$. The amount of anhydrous acetic acid used in the synthesis of binary oxide gel system was the same as that used for the silicon dioxide gel (5.25 mol), but in the synthesis of each subsequent sample; the amount of the acetate ions was reduced by a value already included in lanthanum (III) acetate. The gel was dried at 393 K by slow evaporation from the vessel with the gel, for 72 h, which permitted formation of a stable monolith.

Thermal analysis

Thermal transformation of the gel samples was recorded on a SETSYS 12 (Setaram, France) under the same conditions. A 20 mg sample was placed in alumina crucibles (volumes—100 mm^3) and heated at the rate of 5 K min^{-1} up to 1373 K. For all experiments, we used the fraction of the grain sizes between 100 and 200 Mesh. The above fraction was set apart from the powder obtained in agate grinder. The TA–TG curves of each sample were recorded in the air atmosphere.

X-ray diffraction analysis

All the samples were identified by powder XRD using a D8 Advance Diffractometer made by Bruker with the copper $K_{\alpha 1}$ radiation ($\lambda = 1.5406$ Å). The XRD patterns were recorded at the room temperature, in the 2-theta range 6°–60° by step scanning, using 2-theta increments of 0.04° and fixed counting time of 2 s/step.

Porous structure

The porous structure was determined by the low-temperature (77 K) nitrogen adsorption measurements carried out on the accelerated surface area and a porosimetry system model 2010 V2.00 D made by Micromeritics, using 200–300 mg of material fraction of grain size between 0.1 and 0.2 mm. Prior to nitrogen adsorption, all samples were outgassed at 623 K at 0.4 Pa till constant weight. Both adsorption and desorption branches of the isotherm were taken in the p/p_0 range 0–1. Adsorption measurements were performed on the gel samples preheated in O_2 atmosphere for 8 h at 773 K.

FTIR investigation

FTIR transmission spectra were recorded at room temperature on a Bruker IFS88 Spectrometer (128 scans) in the 4000–400 cm^{-1} wavenumbers range. In order to explore with a suitable resolution the region 400–1000 cm^{-1}, the spectra were recorded after dispersion in KBr matrix. The samples heated in O_2 atmosphere for 8 h at 200, 400, and 600 °C were pressed into self-supporting discs (2 mg of finely ground material in 200 mg of KBr).

Results and discussion

The X-ray diffraction studies were performed for samples of various compositions to identify the components formed during the thermal treatments. The XRD patterns of SiO_2–La_2O_3 samples calcined at 500 °C in atmosphere of oxygen
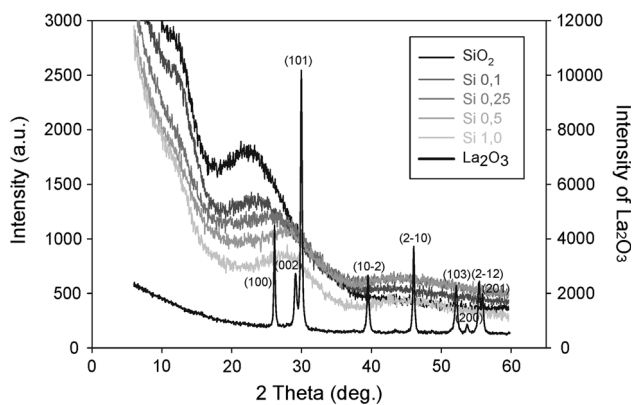
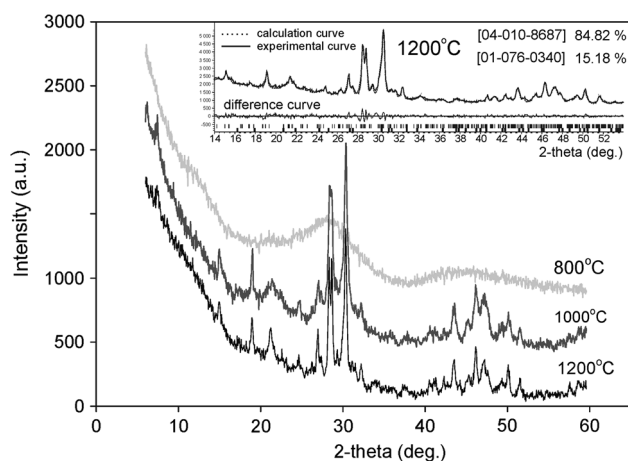**Fig. 1** XRD measurements of SiO$_2$–La$_2$O$_3$ samples calcined under oxygen at 500 °C

Fig. 2 XRD patterns of SiLa 1.0 sample calcined under air at 800, 1,000 and 1,200 °C. X-ray Rietveld plot of a two phase refinement of La$_6$Si$_4$(SiO$_4$)$_2$O$_{13}$ and La$_{9.31}$(Si$_{1.04}$O$_4$)$_6$O$_2$ is given in the *inset*

are presented in Fig. 1. The X-ray diffraction scans of silicon dioxide and binary oxide system proved that the samples had amorphous nature even for the largest quantity of lanthanum used. Amorphous phases cannot be detected directly by X-ray diffraction analysis, because they do not produce additional visible reflexes in the XRD diagram, but only increase the background and wide range halo. Meanwhile, the lanthanum oxide showed eight characteristic peaks, which are indexed on the basis of a hexagonal unit cell with the lattice parameters of a = 3.94094(21)Å, c = 6.13207(35)Å, and the space group of a P-3m1 [22, 23]. The SiLa 1.0 (ratio Si/La 1:1) sample treated at 800, 1000 and 1200 °C (Fig. 2), crystallized in two oxides: monoclinic lanthanum silicon silicate oxide, La$_6$Si$_4$(SiO$_4$)$_2$O$_{13}$, [04-010-8687] and hexagonal lanthanum silicate oxide La$_{9.31}$(Si$_{1.04}$O$_4$)$_6$O$_2$, [01-076-0340]. The structure refinements were performed using the program

FullProf [24]. Crystalline phase identification was carried out using the diffractometer analytical software after revision of the PDF4 + (2011) 4.11.0.3 ICDD database crystalline compounds [25].

The TG–DTG–TA curves of the SiO$_2$–La$_2$O$_3$ samples are shown in Fig. 3 and evidence mass loss at three consecutive steps (at about 390, 630 and 660 K). The results obtained from the range 300–1373 K indicate that all samples have a quite similar content of organic product matter. The first endothermic peak at 390 K is attributed to the evaporation process of acetate acid, in compliance with the first mass loss marked on TG curves. The next two exothermic peaks at 630 and 660 K, are very difficult to interpret, they are supposedly due to the combustion of ethyl acetate and acetate acid as shown by the analysis of CO$_2$$^+$ ($m/z = 44$) ions abundance as function of temperature [14].

The main aim of FTIR investigation was to confirm the formation of Si–O–Si and Si–O–La bonds in the gel structure. According to our earlier investigation of the SiO$_2$–SnO$_2$ system [19], the most prominent region for silica-based materials lies between 900 and 1400 cm^{-1} and is connected to the stretching vibration of the Si–O–Si network. The characteristic peak and shoulder seen at approximately 1081 and 1195 cm^{-1} were assigned to the asymmetric stretching vibration of the three-dimensional Si–O–Si network. Both are assigned to the same vibration, however, the maximum at 1081 cm^{-1} could be assigned to the transverse optical mode of the asymmetric vibration, while the shoulder around 1200 cm^{-1} could be assigned to the longitudinal optical mode. The symmetric stretching vibration of the Si–O–Si network is manifested as the band at around 800 cm^{-1} [26, 27] and in the spectrum of pure SiO$_2$ gel sample it appears at 801.6 cm^{-1} (Fig. 4, for the gel dried at RT). Higher temperature of gel calcination is responsible for a shift of the bands corresponding to both types of stretching vibrations towards higher wavenumber values (Fig. 4). It has been proposed [26] that this shift reflects an increasing rigidity of the Si–O–Si network as condensation occurs. Thus, for example, the position of to v_{asym} shifts from 1074.5 cm^{-1} (for the gel dried at RT) to 1089.6 cm^{-1} for the SiO$_2$ sample calcined at 600 °C. Per analogy, the position of the peak corresponding to the symmetric stretching vibration of Si–O–Si shifts from 801.6 cm^{-1} (for the gel dried at RT and 200 °C) to 805.8 cm^{-1} (400 °C) finally to 810.1 cm^{-1} for the sample calcined at 600 °C. The band appearing at about 460 cm^{-1} is associated with the bending mode of Si–O–Si. This band undergoes a shift upon an increase in the heat treatment temperature, but this shift is not as tangible as that assigned to the stretching vibrations. The maximum of this band occurs at 458.5 cm^{-1} for the samples of incompletely developed network structure (the samples dried at room
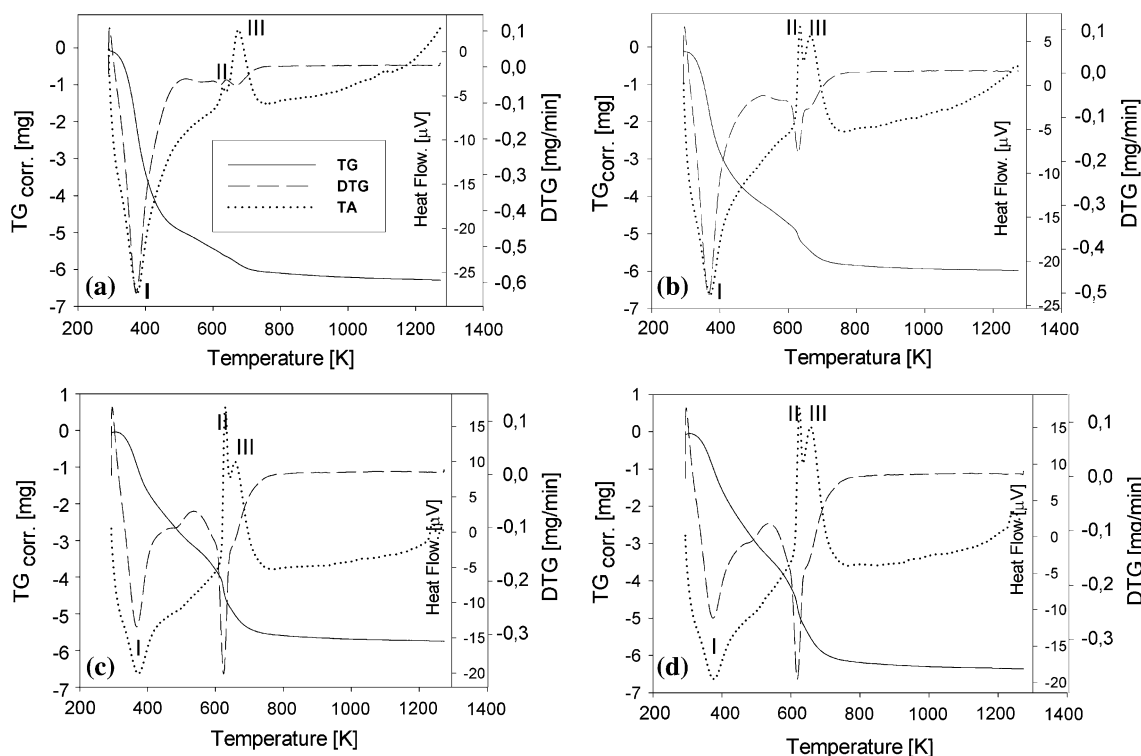
Fig. 3 TG–DTG–TA curves for **a** SiLa 0.1, **b** SiLa 0.25, **c** SiLa 0.5, **d** SiLa 1.0 in the air atmosphere up to 1,373 K

temperature). It is worth noting that the temperature factor changes the position of the maxima from 462.0 by 462.4 to 462.7 cm^{-1}, for the samples calcined at 200, 400 and 600 °C, respectively. According to literature [26, 27] the band with a maximum at around 960 cm^{-1} could be assigned to surface Si–O$^-$ groups. As expected, the intensity of this band decreases with the increasing temperature of gel treatment (Fig. 4). Finally, for the gel calcined at 600 °C a band is no longer discernible and becomes an inflection point on the curve. Considering the possibility of formation of Si–O–La bonds in the gel structure, the most interesting part of IR spectrum is connected to the bands appearing in the IR spectrum of SiO$_2$ around 1080, 800 and 460 cm^{-1}. The shift of the signal characteristic of Si–O–Si stretching vibrations to lower frequencies could be a result of introduction of a second metal oxide [26]. A reasonable explanation of the above displacements to lower frequencies is a weakening of the Si–O–Si bonds. According to Parler [28], this shift to lower wave numbers implied a reduction in the vibrational energy, and hence a reduction in the strength of the bonds comprising the silicon–oxygen backbone structure of the mixed-metal oxides. As follows from the above, the addition of high amounts of the second metal resulted in an overall weakening of the original silica gel network. Figure 5 shows the spectra of the binary oxide gel system SiO$_2$–La$_2$O$_3$, calcined at 600 °C. Incorporation of lanthanum into the gel matrix induces the shifts of the signals

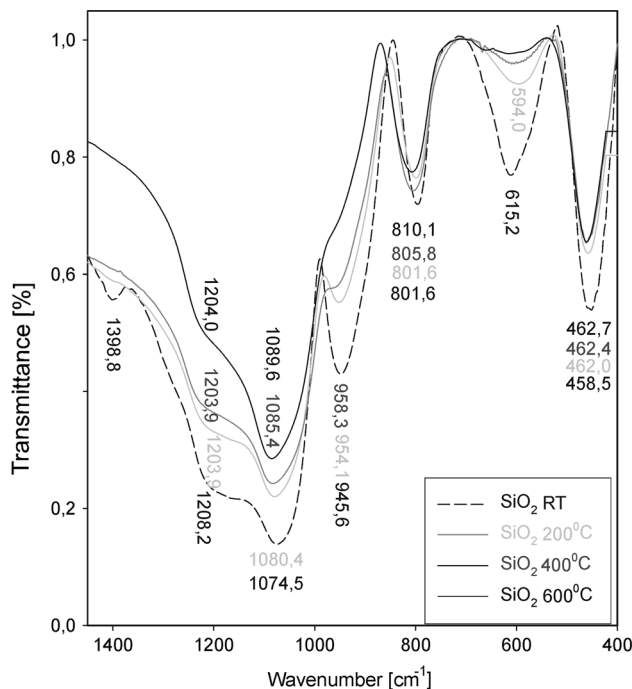

Fig. 4 Effect of calcination at temperatures of 200, 400 and 600 °C on the position of the IR bands in the SiO$_2$ gel sample prior to being formed into a KBr pellet + RT

assigned to the asymmetric stretching vibration (1080 cm^{-1}) and the symmetric stretching vibration (800 cm^{-1}) of Si–O–Si towards lower frequencies. The
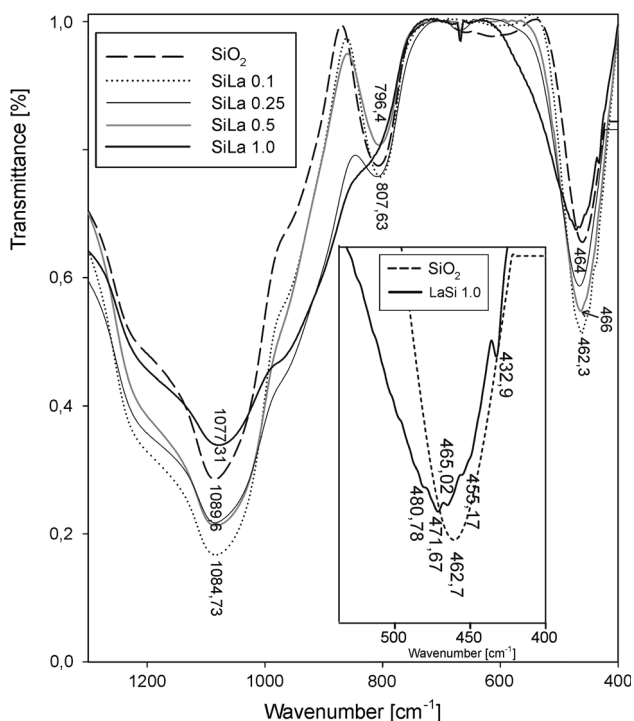
Fig. 5 Position of the IR bands as a function of concentration of lanthanum in the SiO_2–La_2O_3 system calcined at 600 °C. Samples dispersed in KBr matrix. *Inset* zoom of the region between 400 and 550 cm^{-1}
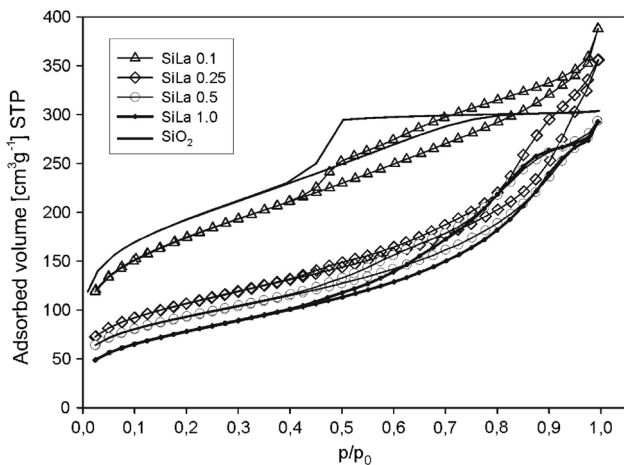

Fig. 6 Changes in the nature of the adsorption–desorption isotherms associated with the increasing content of La_2O_3 in the mass binary oxide gel system

Fig. 7 Comparison of the distribution of pore volume for systems with a small (a) and a large amount (b) La_2O_3, in the binary oxide system

maximum of the former band shifts from 1,089.6 cm^{-1} (SiO_2 gel) to 1084.73, 1079.9, 1078.2, 1077.31 cm^{-1} for SiLa 0.1, SiLa 0.25, SiLa 0.5 and SiLa 1.0, respectively. Similarly, the band occurring at 807.63 cm^{-1} (SiO_2 gel) is shifted to 804.18, 796.5, 796.4 cm^{-1}, for the samples with La_2O_3 contents 0.1, 0.25 and 0.5. Finally, for the system with a maximum concentration of La_2O_3 (SiLa 1.0) this
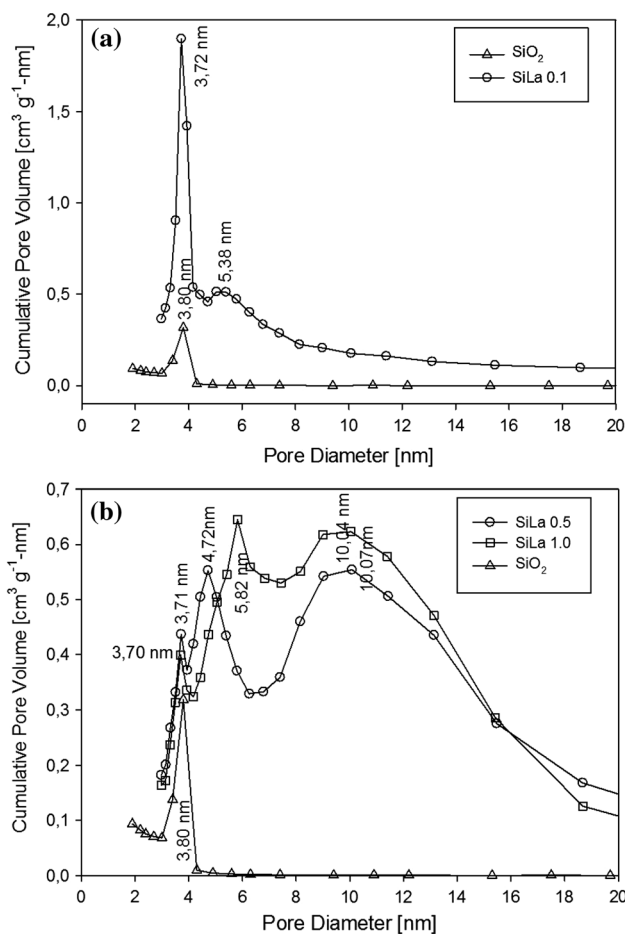
band appears only as an inflection point. La_2O_3 incorporation into the gel samples leads to a shift of the band associated with the bending mode of Si–O–Si (462.7 cm^{-1}, SiO_2 gel) towards higher wave numbers. The maximum of this band occurs at 462.3, 464.0 and 466.0 cm^{-1} for the samples SiLa 0.1, SiLa 0.25 and SiLa 0.5, respectively. For the sample with the highest amount of the second component (SiLa 1.0) in the spectrum, we were able to observe poorly distributed band with a group of peaks at 432.9, 455.17, 465.02, 471.67 and 480.78 cm^{-1} (Fig. 5, inset).

Results of the textural analysis obtained for selected samples of this series are presented in Figs. 6 and 7. For the majority of samples, the isotherm recorded is of the IV type, and it is accompanied by a H2-type hysteresis loop. Only for pure SiO_2 gel (Fig. 6), the character of the isotherm is of mixed IV and I type. As type I isotherm corresponds to the solid phase with microporous structure, the pure silica gel should also include micropores besides the mesopores indicated by type IV isotherm (the isotherm type IV accompanied with the H2 hysteresis loop is associated with capillary condensation taking place in

Table 1 Texture parameter for mono and binary gel samples

Sample	Molar ratio $SiO_2:La_2O_3$	S_{BET} (m^2 g^{-1})	Cumulative pore volume of mesopores[a] (cm^3 g^{-1})	Micropore volume[b] (cm^3 g^{-1})	Average pore diameter (nm)
SiO$_2$	1:0	682	0.341	0.460	2.74
SiLa 0.1	1:0.1	591	0.601	0.208	4.08
SiLa 0.25	1:0.25	364	0.551	0.062	5.85
SiLa 0.5	1:0.5	318	0.455	0.036	5.73
SiLa 1.0	1:1	279	0.454	0.000	6.51

[a] Pores with diameter less than 350 nm

[b] On the base of *t*-plots

mesopores). The above hypothesis has been supported by the results obtained by the method proposed by Lippens-de Boer (*t*-plots) that have proved the presence of micropores. This applies particularly to SiO$_2$ gel and binary oxide gel systems with small amounts of lanthanum oxide (SiLa 0.1), where the micropore volume calculated from *t*-plots was the largest. A further increase in the concentration of the second oxide, leads to a clear decrease in the amount of micropores in the gel system (see Table 1), finally, no evidence of their presence in the sample SiLa 1.0 was detected (from *t*-plot). Therefore, the reduction of micropores in the gel structure implies an increase in the average pore radius.

As follows from the numerical data compiled in the Table 1, the surface areas of the silicon dioxide gel and binary oxide gel system, differ significantly. In the entire concentration range of lanthanum oxide additive introduced, its presence led to a gradual reduction in the surface area. The surface area of sample SiLa 1.0 is about twice smaller than that for the unmodified silica gel pure SiO$_2$ gel. It should be noted that the introduction of the modifier (La$_2$O$_3$) causes an increase in the total pore volume, which is much higher for the modified than for the unmodified silica gel. This may be a consequence of the fact that in addition to mesopores, similarly as in the unmodified silica, pores with large diameters appear. Thus, a consequence of introduction of an additive is a change in mono-modal population of mesopores characteristic of the unmodified gel. In the binary oxide system, the additive introduced led to generation of a range of pores with larger diameters (Fig. 7).

Conclusions

The surface properties of binary SiO$_2$–La$_2$O$_3$ oxide system prepared by non-aqueous sol–gel method were studied. The use of acetic acid as a solvent and reagent permits obtaining a simpler sol–gel system and allows synthesis of organic–inorganic materials from the components insoluble in polar medium. The X-ray powder patterns verified the amorphous structure of Si/La binary oxide gel system investigated in this work. A large decrease in the surface

area and micropore volume were noted with the increasing lanthanum substitution in the gel network. On the other hand, the average pore diameter increases with the increasing content of La in the SiO$_2$–La$_2$O$_3$ system. FTIR spectra data show that La incorporation into the gel leads to a shift of the band assigned to the bending mode of Si–O–Si towards higher wavenumbers.

References

1. Que WX, Kam CH, Zhou Y, Lam YL, Chan YC (2001) Yellow-to-violet upconversion in neodymium oxide nanocrystal/titania/ormosil composite sol–gel thin films derived at low temperature. J Appl Phys 90:4865–4867
2. Yamamoto T, Matsuyama T, Tanaka T, Funabiki T, Yoshida S (1999) Generation of acid sites on silica-supported rare earth oxide catalysts: structural characterization and catalysis for α-pinene isomerization. Phys Chem Chem Phys 1:2841–2849
3. Rieck JS, Bell AT (1986) Studies of the interactions of H$_2$ and CO with PdSiO$_2$ promoted with La$_2$O$_3$, CeO$_2$, Pr$_6$O$_{11}$, Nd$_2$O$_3$, and Sm$_2$O$_3$. J Catal 99:278–292
4. Mista W, Zawadzki M, Grabowska H (1996) Formation of neodymium-aluminium oxide binary system prepared from nitrates by coprecipitating with ammonia. Pol J Chem 70:1506–1511
5. Berkessel A, Ashkenazi E, Andreae MRM (2003) Discovery of novel homogeneous rare earth catalysts by IR-thermography: epoxide opening with alcohols and Baeyer–Villiger oxidations with hydrogen peroxide. Appl Catal A254:27–34
6. Andriamasinovo D, Kieffer R, Kiennemann A (1993) Preparation of stabilized copper-rare earth oxide catalysts for the synthesis of methanol from syngas. Appl Catal A106:201–212
7. Bazzi R, Flores-Gonzales MA, Louis C, Lebbou K, Dujardin C, Brenier A, Zhang W, Tillement O, Bernstein E, Perriat P (2003) Synthesis and luminescent properties of sub-5-nm lanthanide oxides nanoparticles. J Lumin 102:445–450
8. Jothinathan E, Vanmeensel K, Vleugels J, Van der Biest O (2010) Synthesis of nano-crystalline apatite type electrolyte powders for solid oxide fuel cells. J Eur Ceram Soc 30:1699–1706
9. Rodrıguez-Reyna E, Fuentesa AF, Maczkab M, Hanuzab J, Boulahyad K, Amadore U (2006) Facile synthesis, characterization and electrical properties of apatite-type lanthanum germanates. Solid State Sci 8:168–177
10. Brinker CJ, Scherer GW (1990) Sol-gel science: the physics and chemistry sol–gel processing. Academic Press, New York

11. Sharp KG (1994) A two-component, non-aqueous route to silica gel. J Sol–Gel Sci Technol 2:35–41
12. Khimich NN, Venzel BI, Koptelova LA (2002) Fabrication of monolithic silicon gel in a nonaqueous medium doklady. Phys Chem 385(4–6):201–202
13. Khimich NN, Venzel BI, Koptelova LA, Drozdova IA (2002) Acetic acid in sol–gel process of hydrolytic polycondensation of tetramethoxysilane russ. J Appl Chem 77(2):294–298
14. Kirszensztejn P, Kawałko A, Tolińska A, Przekop R (2011) Synthesis of SiO$_2$–SnO$_2$ gels in water free conditions. J Porous Mater 18:241–249
15. Wachowski L, Kirszensztejn P, Lopatka R, Bell TN (1995) Studies of physicochemical and surface properties of alumina modified with rare earth oxides. Cat Lett 32:123–130
16. Wachowski L, Kirszensztejn P, Lopatka R, Czajka B (1994) Studies of physicochemical and surface properties of alumina modified with rare-earth oxides I. Preparation, structure and thermal stability. Mater Chem Phys 37:29–38
17. Zhang X, Walters AB, Vannice MA (1995) NO adsorption, decomposition, and reduction by methane over rare earth oxides. J Catal 155:290–302
18. Gliński M, Kijeński J, Jakubowski A (1995) Ketones from monocarboxylic acids: catalytic ketonization over oxide systems. Appl Catal A128:209–217
19. Dollimore D, Pearse J (1980) Nitrogen adsorption isotherms on porous powders of alumina and silica coated with manganese oxides. Powder Technol 25:71–78
20. Zhang X, Walters AB, Vannice MA (1994) NO$_x$ decomposition and reduction by methane over La$_2$O$_3$. Appl Catal B4:237–256
21. Zheng X, Lin H, Zheng J, Duan X, Yuan Y (2013) Lanthanum oxide-modified Cu/SiO$_2$ as a high-performance catalyst for chemoselective hydrogenation of dimethyl oxalate to ethylene glycol. ACS Catal 3:2738–2749
22. Hu C, Liu H, Dong W, Zhang Y, Bao G, Lao C, Wang ZL (2007) La(OH)$_3$ and La$_2$O$_3$ nanobelts-synthesis and physical properties. Adv Mater 19:470–474
23. Salavati-Niasaria M, Hosseinzadeh G, Davar F (2011) Synthesis of lanthanum hydroxide and lanthanum oxide nanoparticles by sonochemical method. J Alloys Compd 509:4098–4103
24. Rodriguez-Carvajal J (1993) Recent advances in magnetic structure determination by neutron powder diffraction. Phys B 192:55–69
25. JCPDS Powder Diffraction File International Centre for Diffraction Data, 12 Campus Boulevard, Newtown Square, PA, USA. 19073-3273
26. Perry CC, Li X, Waters DN (1991) Structural studies of gel phases—IV. An infrared reflectance and Fourier transform Raman study of silica and silica/titania gel glasses. Spectrochim Acta 47A:1487–1494
27. Cordoba G, Arroyo R, Fierro JLG, Viniegra M (1996) Study of xerogel–glass transition of CuO/SiO$_2$. J Solid State Chem 123:93–99
28. Parler CM, Ritter JA, Amirdis MD (2001) Infrared spectroscopic study of sol–gel derived mixed-metal oxides. J Non Cryst Solids 279:119–125